© Wydawnictwo UR 2017
ISSN 2544-1361 (online); ISSN 2544-2406
doi: 10.15584/ejcem.2017.2.3

http://www.ejcem.ur.edu.pl/en/
European Journal of Clinical and Experimental Medicine
Eur J Clin Exp Med 2017; 15 (2): 109–119

REVIEW PAPER

Zuzanna Bober [1(ABGF)], David Aebisher [2(ABF)], Łukasz Ożóg [3(F)], Jacek Tabarkiewicz [1,2(F)], Piotr Tutka [1,4(F)], Dorota Bartusik-Aebisher [4(ABF)]

^{19}F MRI As a tool for imaging drug delivery to tissue and individual cells

[1] Center for Innovative Research in Medical and Natural Sciences, Faculty of Medicine, University of Rzeszow, Rzeszow, Poland
[2] Department of Human Immunology, Faculty of Medicine, University of Rzeszow, Rzeszow, Poland
[3] Department of Biophysics, Faculty of Mathematics and Natural Sciences, University of Rzeszow, Rzeszow, Poland
[4] Department of Experimental and Clinical Pharmacology, Faculty of Medicine, University of Rzeszow, Rzeszow, Poland

ABSTRACT

Over the past few decades, magnetic resonance imaging (MRI) has proven to be extremely successful in medical applications. More recently, the biomedical applications of MRI have been gaining more use in the field of clinical pharmacy. In 1977, perfluorocarbon compounds (PFC), which form emulsions that can carry drugs, were analyzed by ^{19}F MRI and emulsified PFC compounds have been investigated as potential blood substitutes since the early 1960s and now a wide variety of PFC compounds are currently available as ^{19}F MRI biomarkers. Molecules with ^{19}F substituents are particularly attractive for use in drug tracking by ^{19}F MRI due to 100% ^{19}F abundance, high ^{19}F MRI sensitivity (0.83 relative to ^{1}H MRI) and an impressively large chemical shift range (400 ppm). Another benefit in the use of ^{19}F MRI is a zero background signal in biological samples due to lack of endogenous fluorine. Therefore, drugs containing fluorine atom have potential for ^{19}F MRI imaging drug delivery to tissue. This article will review recent developments in the use of ^{19}F MRI in imaging drug delivery to tissue and individual cells.

Keywords. drug delivery, drug tracking, fluorine, magnetic resonance imaging

Introduction

In this review, we will cover recent publications on fluorine-19 (^{19}F) Magnetic Resonance Imaging and Spectroscopy, ^{19}F ralaxation time, contrast agents, drug delivery, oxygen concentration in tumor tissue and individual cells. Our interest is in review of ^{19}F MRI applications to study cancer cells and cancer drug efficacy *in vitro*. Our focus is to present study that trying to explore cellular aspect of cancer by ^{19}F MRI techniques, so that an anti-tumor drug containing ^{19}F can not only be delivered to the cell, but also released inside the cell itself and constantly monitored. Current drug targeting research shows posibility

Corresponding author: Dorota Bartusik-Aebisher, e-mail: dbartusik-aebisher@ur.edu.pl

Participation of co-authors: A – Author of the concept and objectives of paper; B – collection of data; C – implementation of research; D – elaborate, analysis and interpretation of data; E – statistical analysis; F – preparation of a manuscript; G – working out the literature; H – obtaining funds

Received: 22.02.2017 | Accepted: 24.04.2017
Publication date: June 2017

Bober Z, Aebisher D, Ożóg Ł, Tabarkiewicz J, TutkaP, Bartusik-Aebisher D. *^{19}F MRI As a tool for imaging drug delivery to tissue and individual cells.* Eur J Clin Exp Med. 2017;15(2):109–119. doi: 10.15584/ejcem.2017.2.3

of limiting the side effects of the drugs and ultimately improving cancer treatment. However, when MRI is used for *in vitro* cell culture studies will require a high concentration of cells (order of 10^8 cell/mL).

^{19}F MRI techniques are valuable for non-invasive and non-destructive monitoring of fluorine biopharmaceuticals. There is an urgent need for cost-effective, non-invasive diagnostic techniques for monitoring the location of anticancer drugs due to their high toxicity in non-diseased tissue. While contrast-enhanced MRI can provide high sensitivity for the detection, ^{19}F MRI can provide much higher contrast due to lack of tissue background. ^{19}F MRI can characterize the biophysical states of ^{19}F in tissue and tissue perfusion by relaxation time measurements. In studies on many drug interactions in the tissue, the application of ^{1}H MRI has been limited because of the large molecular mass of water results in very broad signals. However, ^{19}F MRI can be used to aid pharmacodynamics and pharmacokinetics of several medically important fluorinated drugs. A wide range of chemical shift for the ^{19}F nucleus ensures good separation of signals in different environments. ^{19}F MRI offers an quantitative way of *in vitro* imaging high ^{19}F MRI sensitivity (0.83 relative to ^{1}H MR), an impressively large chemical shift range (~400 ppm) and zero background signal in biological samples. ^{19}F MRI a reliable analytical tool for monitoring organofluorine compounds and their quantification, when an internal standard of known concentration is included without the need for separation and derivatization steps. Importantly, such ^{19}F NMR studies translate well into a clinical setting as ^{19}F MRI allows the noninvasive monitoring of drug metabolism and pharmacokinetics. With the aim to investigate drug ^{19}F MRI and MRS we search literature data bases to find innovative applications for our study. Both techniques, ^{19}F MRI and ^{19}F MRS, can be used to examine structural aspects of much higher molecular weight proteins, which traditional one- or multi-dimensional NMR experiments fail to resolve. Many medicines containing fluoride compounds are available on the market and they are still growing.[1] Attention should be drawn to the possibility of analyzing ^{19}F spectra of drugs in both *in vivo* and *in vitro* studies focusing on ^{19}F of physiological fluids such as blood plasma. Developing such a method would allow for the observation of drug metabolism and dosage control. Perfluorocarbons (PFCs) are chemical compounds in which hydrogen atoms replace fluorine atoms. Emulsion-forming PFC compounds are used as the drug carrier analyzed by ^{19}F MRI. A 5-fluorouracil (5-FU), was the first anticancer drug introduced in 1957.[2] 5-FU is an antimetabolite cytostatic and a thymine derivative where the C-5 methyl group is replaced by the ^{19}F atom. In 1977, PFC which are contrast emulsions that can carry drugs, were analyzed by ^{19}F MRI.[3] PFC compounds are an potential blood substitutes and they are investigated since the early 1960s.[4] In 2005, it was shown for the first time by Ahrens et al. that cells can be labelled with PFC emulsions and tracked *in vivo* by ^{19}F MRI.[5] Below is a graph showing the number of ^{19}F MRI publications in the PubMed database over the years starting from 1885.

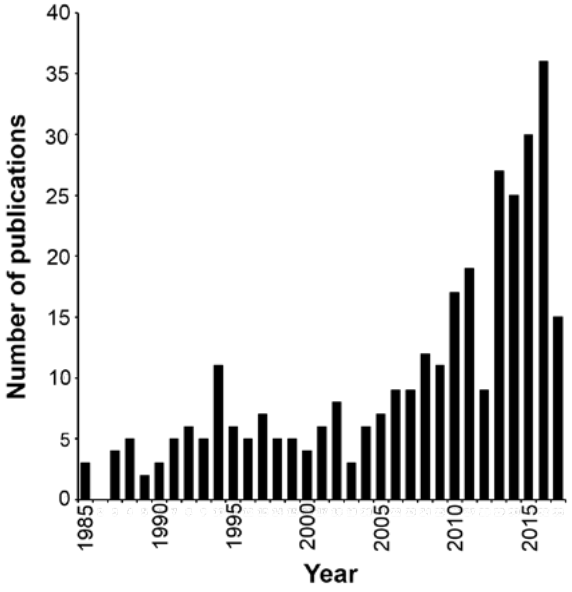

Figure 1. Number of publications on ^{19}F MRI collected from Library of National Center for Biotechnology Information (NCBI) PubMed Data Base

Among various types of imaging, ^{19}F MRI can provides a useful analytical tool to determine the localization of ^{19}F in the tissue. As the fluorine nuclei is normally absent in tissues, there is no natural abundance background. From all types of spectroscopy, ^{19}F MRS can provide signal and allows to quantify signal intensity. In MRS measurement of the spectrum is measured using a MRI scanner. The use of ^{19}F MRI and MRS has scientific and clinical significance. Both techniques can be used to measure specific drug concentrations, drug targeting and pharmacokinetics. Results obtained has helped to unveil how drugs work, why and which patients are non-responders, and aids modern individualized medicine. The most known examples of ^{19}F MRS are applications to measure the pharmacokinetics of drugs at their target sites are illustrated in many articles by human studies with 5-FU.[6] There is a direct relationship between tumor drug uptake and efficacy of therapy.[7]

Recently, micelles of tetraethylammonium perfluorooctanesulfonate (TPFOS, $C_8F_{17}SO_3N(C_2H_5)_4$, aqueous solutions of $C_9F_{19}COON(CH_3)_4$, fluoro- and hydrocarbon surfactants with different tail lengths and counterions ($^+N(CH_3)_4$, $^+N(C_3H_7)_4$ Li^+ and Na^+) have been studied by using ^{19}F MRS.[8] ^{19}F labeled phenolic compounds in early stages of oxidation of edible oils based on the formation of α-tocopheryl radicals initiated by oil-soluble vanadium complexes was studied.[9] The study by Hu and coworkers

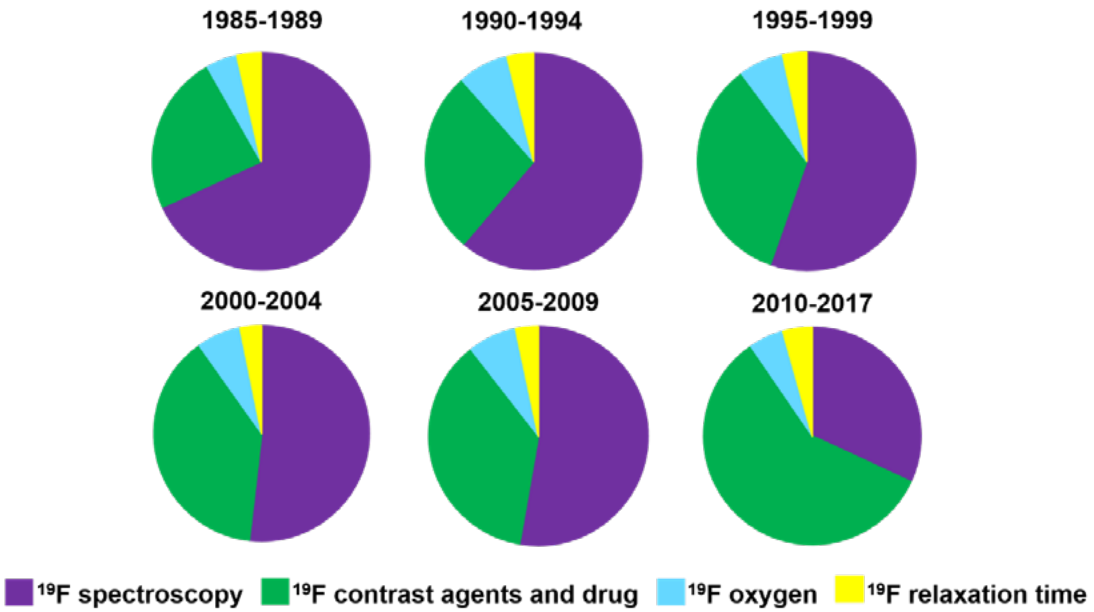

Figure 2. The statistic of [19]F research collected from Library of National Center for Biotechnology Information (NCBI) PubMed Data Base

have been demonstrated that [19]F NMR can be used as an alternative method to conventional radiolabeled studies for compounds containing fluorine without the need for radiolabeled synthesis.[10] Therefore, monitoring of tumor drug metabolism can separate responders form non-responders and thus prevent unnecessary toxicity. Possible to identify patients likely to respond to 5-FU. Capecitabine is designed as a pro-drug of 5-FU that can be taken orally; it is used as primary or adjuvant therapy in a range of cancers. Capecitabine metabolism in humans, and especially its heterogeneity, can be non-invasively assessed in the same manner. In addition, [19]F spectroscopy, [19]F contrast agents and drug [19]F oxygen and [19]F relaxation time were grouped. Figure 2 below shows the percentage distribution of topics in each year during 1985-2017.

[19]F contrast agents and drugs

Fluoroorganic and fluoroinorganic compounds are very rare in nature and the few do occur in nature are highly toxic. The reaction to introduce [19]F to compounds is called fluorination. Examples of popular organofluoroxy reagents are acetyl hypofluorite which was used to fluorinate aromatic rings[11] and acetyl hypofluorite which has been intensively studied to use for addition to double bonds[12], fluorination of lithium enolates[13], and synthesis of α-fluorocarboxylic acid derivatives.[14] Another group the *N*-fluoropyrimidium triflates have been used to fluorinate aromatic rings, carbanions, enol ethers and their derivatives.[15]

As mentioned on above Figure 2, [19]F MRS has contributed to the development of agents modulating tumor drug metabolism. To date, the review of literature showed a research done with 5-FU[16], NaF[17-18], lescol[19], flunarizinum[20], mirenil[21], fevarin[22], sevofluran[23], cisprofloxacin[24], haloperidol[25], prozac[26], ciprinol flumetasone[27], perfluorodecalin[28] and trastuzumab[29]. To obtain a quantitative estimate of the drug, [19]F MRS is neccesary to study dynamic abundance of [19]F. In addition to the [19]F drugs, ongoing research is underway to find effective marker cells in [19]F MRI. Therapeutic cells are usually marked with MRI contrast agents, including gadolinium ions (Gd^{3+}), super paramagnetic iron oxides (SPIO) nanoparticles, or fluorinated compounds, to enhance the contrast.[30,31] PFCs, are inert and stable and are not part of any molecular pathway. Also, [19]F is known as a creator of a strong contrast signal *in vitro* and *in vivo* in background-free samples or tissue. *In vivo* [19]F MRS measurements of trifluorinated neuroleptics such as fluphenazine and trifluoperazine and antidepressants such as fluoxetine and fluvoxamine began in 1983. The experiment was performed using rats which have been treated with high oral doses of fluphenazine over a period of three weeks and imaged in 10 hours.[32] The reaction between perfluorotoluene and homocysteine thiolactone resulting in the formation of N-substituted homocysteine thiolactone derivative was studied.[33] Ahrens and coworkers describe the first clinical experience using a perfluorocarbon (PFC) tracer agent specifically engineered for [19]F MRI cell detection. Cells are labeled in culture using a PFC nanoemulsion formulation that is taken up by cells regardless of their phagocytic properties.[34] Optimal sensitivity can be achieved with dedicated [19]F compounds together with specifically adapted hardware and acquisition methods.[35] In general, the [19]F labels developed thus far consist of PFCs result-

ing in high ^{19}F density per molecule. PFCs have been proposed as blood substitutes for several decades.[36] ^{19}F MRI in the brains of living mice was published in 2005.[37] Two types of potential imaging agents were developed by using ^{19}F MRI they are ^{19}F-containing curcumin derivatives and ^{19}F-containing styrylbenzoxazole derivatives.[38] F-labeled proteins were used as a proof of concept and initial applications are presented for the HIV-inactivating lectin cyanovirin-N. Single F atoms were introduced at the 4-, 5-, 6- or 7 positions of Trp49 and the 4-position of Phe4, Phe54, and Phe80.[39] Liquid perfluorocarbon nanoparticle contains a high concentration of fluorine eg. 20 equivalent fluorine molecules.[40]

Herceptin efficacy in *ex vivo* cultures of MCF-7 breast carcinoma cells was analyzed.[41] Herceptin was used with perfluorooctyl bromide (PFOB) and conjugated with Lipoplex containing plasmid DNA and Lipofectamine (LipA) to allow ^{19}F MRI studies. Treatments such as Herceptin, Herceptin/PFOB and Herceptin/PFOB/Lipoplex were used for *ex vivo* targeting of MCF-7 cells cultured in three-dimensional (3D) geometry using hollow fiber bioreactor (HFB) device. The viability of MCF-7 cells after 72 h treatments decreased to 54±2%, 50±3% and 45±1% for Herceptin, Herceptin/PFOB and Herceptin/PFOB/Lipoplex, respectively. A significant correlation between the treatment concentration and efficacy was observed in MCF-7 cell cultures.[42] Using the calibration curves for ^{19}F SI, the ^{19}F SI of cells after treatments can be calculated and due to this we can calculate the number of cells targeted by emusions. The calibration curves allowed quantification of the number of fluorine particles bound to cells using the ^{19}F SI. Moreover, using this calibration, we can estimate number of free fluorine particles in media. The ^{19}F SI of PFCE not mixed with Herceptin and other compounds was considered as 100%. The new idea of the research is to synthetize dual probe, test cells labeling and monitor them with ^{19}F MRI/MRS and fluorescence. Drug delivery using dual probes into tumor cells can be accomplished in two steps: first, targeted delivery of drugs to the specific cell, and second, drug targeting inside the cell. The small size agents allow easier delivery to tumor cells as compared to larger or heavier agents. Perfluoropolyetheres (PFPE's) are examples of suitable fluorocarbon ^{19}F MRI agents [5]. Commonly used and useful are cyclic PFPE's such as perfluoro-15-crown-5-ether, perfluoro-18-crown-6-ether and perfluoro-12-crown-4-ether. These compounds can also include additional markers useful for e.g. Positron Emission Tomography (PET) and/or fluorescence. An interesting PFPE is also a linear PFPE. Linear PFPE can relatively easily conjugate a variety of functional entities to the terminal groups. For example, a fluorescent agent attached to the terminal group may be used to generate imaging agents that can be visualized with ^{19}F MRI and fluorescence microscopy.

There are the following 5 options to be considered as dual probes:

1. polyethylene glycols (PEG)+Linear PFPE+polyethyleneimine (PEI) (Figure 3)
2. Linear PFPE+dextran+Cy5.5+antibody (Ab) (Figure 4)
3. Linear PFPE+aminated dextran+Cy5.5+Ab (Figure 5)
4. Fluoresent (Cy5.5) - linear PFPE (Figure 6)
5. Biotinylated ^{19}F compound, FITC dextran, antibody and avidin (Figure 7)

Figure 3 shows the reaction of the terminal groups of polyethylene glycols (PEG) which may be exploited to prepare a range of conjugated imaging reagents. Hydrophilic and lipophilic moieties may be attached to a linear PFPE. PEG can be added to linear PFPE: A-[O--CF_2 (CF_2) x CF_2] n-B where x is an integer from 0 to 10, preferably 0-3, and n is an integer from 2 to 100, preferably 4–40, A–ester and B–amide, amine, forming water-soluble and lipid-soluble conjugates, respectively. Coupling PEG groups to PFPE ester will create a copolymer with water-soluble terminals. We expect that the PEG-PFPE polymer containing water-soluble fluorocarbon and hydrocarbon sections will form micelles with a PFPE core surrounded by PEG. Polyethyleneimine (PEI) can be added during the emulsification process to produce primary, secondary and tertiary amines. These amines in the form of nanoemulsion can be uptaken by tumour cells. The more PEI added into the emulsion, the greater the cellular uptake. ICG will be added during emulsification process.

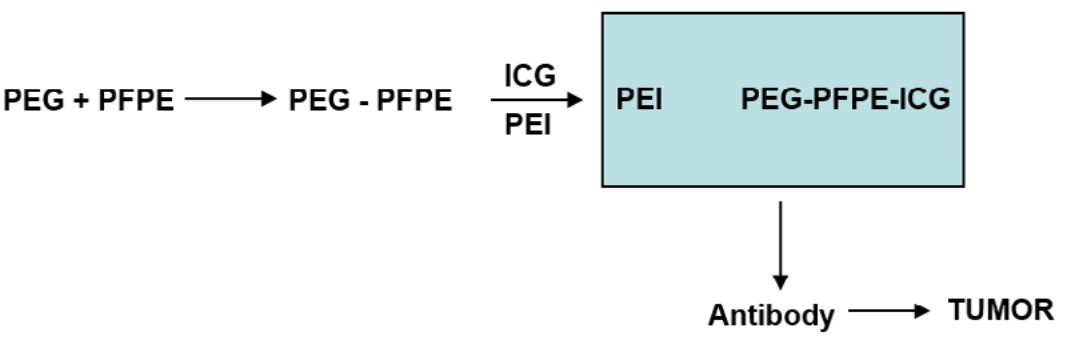

Figure 3. The synthetic scheme of polyethylene glycols (PEG) + Linear PFPE + polyethyleneimine (PEI)

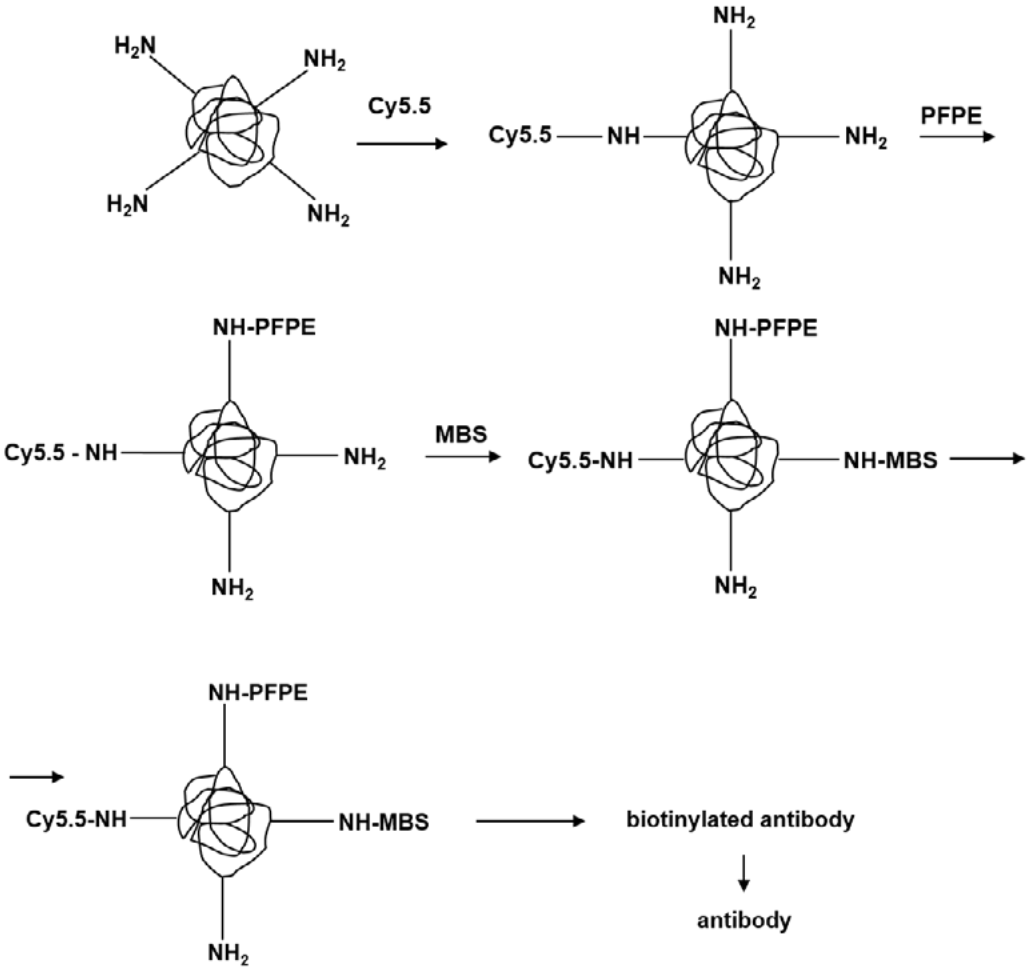

Figure 4. The synthetic scheme of linear PFPE+dextran+Cy5.5+Ab

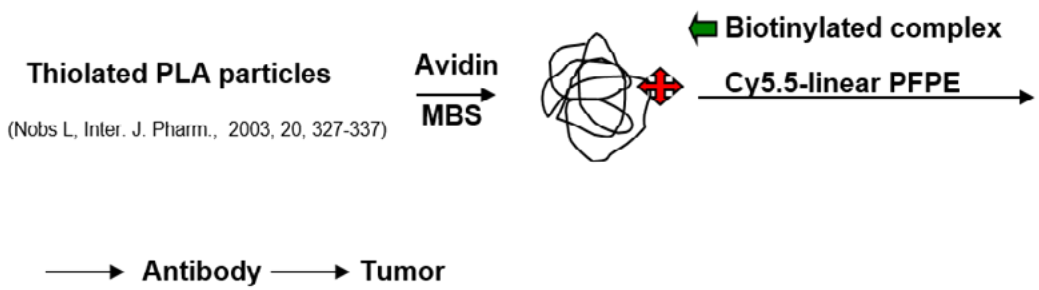

Figure 5. The synthetic scheme of linear PFPE + aminated dextran + Cy5.5+Ab

Figure 4 presents fluorine particles (FP's) consisting of linear PFPE, aminated dextran and Cy5.5. The probe can be modified with sulfo-m-maleimidobenzoyl-N-Hydroxyssicinimide ester (MBS). MBS offer two binding sites; one for primary amino group and one for thiols. Figure 5 shows addition of Avidin and antibody biotinylation.

Figure 6 presents a synthesis which is done by a carbodiimid method[43] followed by the coupling of cystamine dihydrochloride. Next, Avidin can be covalently bounded to the functional PLA particles via the sulfo-MBS. Next, fluoresent (Cy5.5) - linear PFPE particles will be prepared in the following 4 steps: 1) Cy5.5 will be conjugated with aminated dextran; 2) linear PFPE: A-[O--CF_2 (CF_2) x CF_2] n-B will added where x is an integer from 0 to 10, preferably from 0-3, and n is an integer from 2 to 100, preferably from 4 to 40 and A= ester (eg -C(O) O CH_2 CF_3), and B= amide, amine; 3) emulsion will be biotinylated; 4) functional PLA with avidin will be added; 5) Biotinylated antibody will be added and then fluorine particles labeled with avidin can be administrated. Bioti-

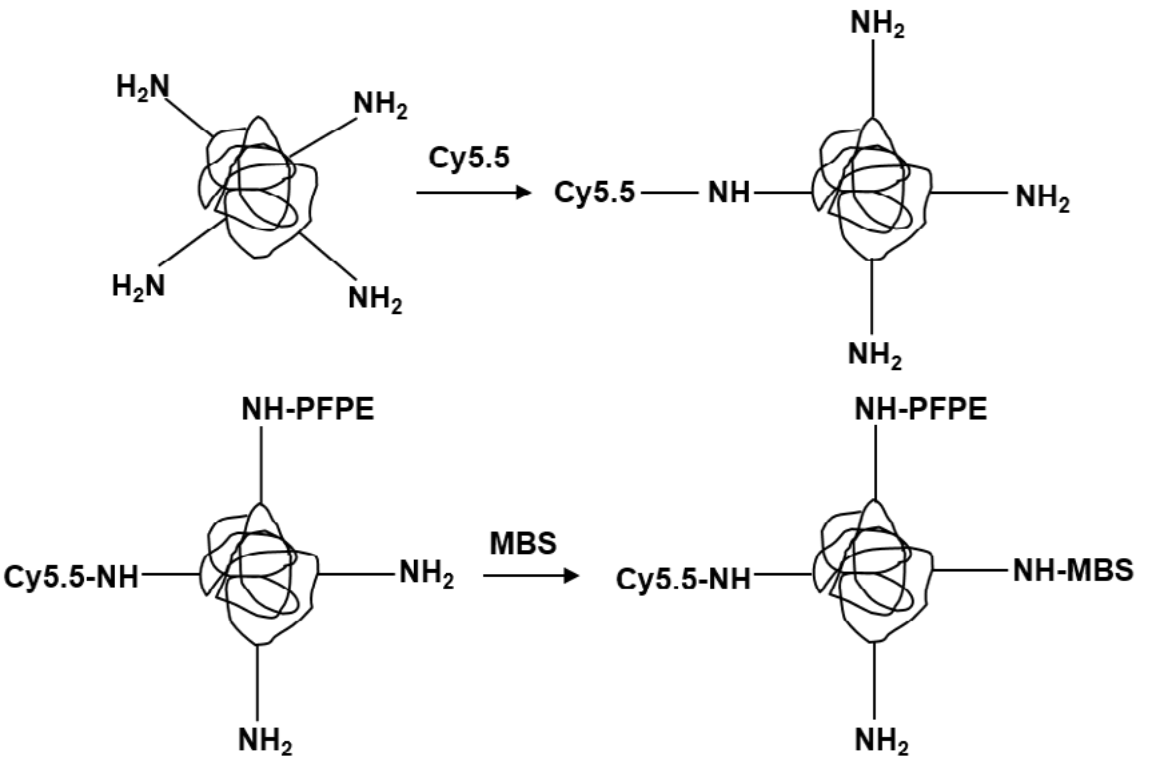

Figure 6. The synthetic scheme of fluoresent (Cy5.5) – linear PFPE

nylated ^{19}F compound, FITC dextran and antibody will be added to avidin.

^{19}F oxygen

Oxygen content in tumor tissue can be monitored with ^{19}F MRI. We hypothesize that the advantage of intracellular O_2 measurements will have an impact on the prophylaxis of cancer. We also expect that the results will provide information on therapeutic procedures involving specific antioxidants in order to improve cancer prevention. Many types of cancers are believed to result from DNA oxidative damage caused by free radicals. Our hypothesis is that antioxidant activity of tocopherols and tocotrienols are involved in the prevention of cellular damage.[44]

A recent clinical study among women using vitamin E supplements provided limited support for the hypothesis that antioxidant supplements may reduce the risk of breast cancer recurrence or breast cancer-related mortality. Antioxidants are substances that prevent damage of cells caused by free radicals.[45] Free radicals are oxygen atoms or chemical molecules with one or more unpaired electrons. Free radicals are usually very unstable and react rapidly with other cell compounds. These free radical reactions are responsible for cell and DNA damage causing possible development of cancer.[46] Vitamin E naturally occurs in four forms: alpha-, beta-, gamma- and delta-tocopherols and four corresponding unsaturated analogues, tocotrienols. The nutritional source of tocopherols and tocotrienols is either diet or vitamin supplements that are based on natural sources such as oil fraction of cereal grains, seeds or nuts. Palm oil is a particularly rich source of tocotrienols.[47] Tocopherols and tocotrienols are antioxidants and are believed to play a preventive role in diseases associated with oxidative stress including cancer.[48] The majority of conducted studies have been mostly focused on the role of alpha-tocopherol, thought to be the most biologically important form of vitamin E in breast cancer.[49] However, observational studies which investigated plasma or adipose tissue concentrations of alpha-tocopherol have failed to consistently support the theory that this isomer provides a protection against breast cancer. Other tocopherols, in particular gamma-tocopherol, have been associated with a reduced incidence of prostate cancer[50] and in a recent study an inhibitory effect on proliferation of prostate cancer cells was reported. Furthermore, delta-tocopherol was demonstrated, in one study, to have inhibitory effects on preneoplastic, neoplastic, and highly malignant mouse mammary epithelial cells whereas alpha- and gamma-tocopherol had no effect on cell proliferation.[51] The role of tocotrienols in cancer research is an important topic for investigators because it has been found that they are potentially active in prevention and treatment of breast, prostate and skin cancer. Recent data indicates that tocotrienols can inhibit proliferation in breast cancer cells. Tocotrienols were proven to protect intact DNA from oxidative stress by inhibition of lipid peroxidation and by binding of reactive free radicals to DNA.[52] The mechanism of action of tocotrienols,

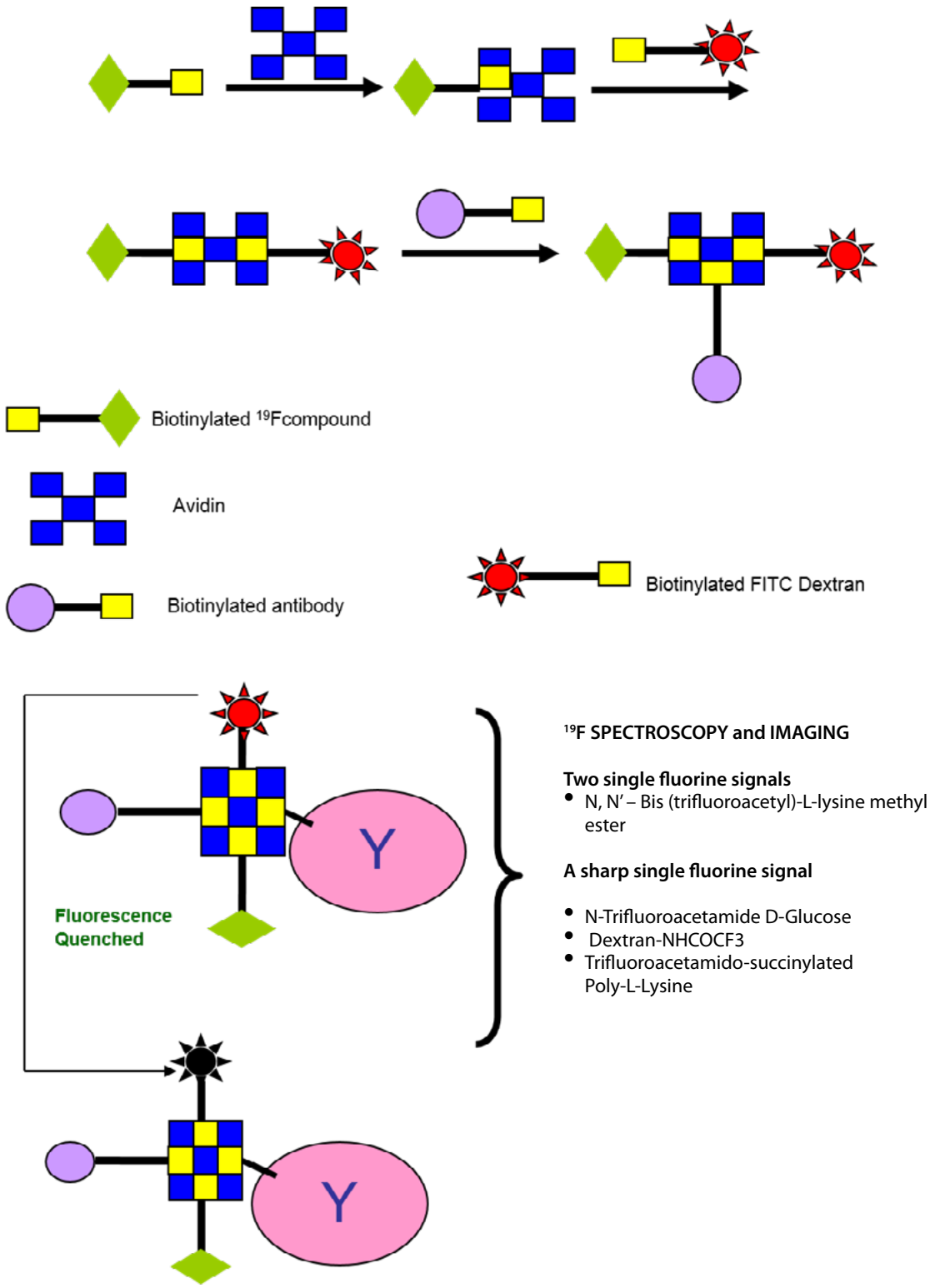

Figure 7. Biotinylated 19F compound constructed from FITC dextran, antibody and avidin

however, is still elusive. Some researchers postulate that the protective role of tocotrienols is not related to their antioxidant properties as shown in a recent study of the effect of tocotrienol-rich fraction from palm oil on gene expression in human breast cancer.[53] The antiproliferative activity of tocotrienols independent of antioxidant properties was also confirmed in a study with lung cancer cells.[54] Moreover, in a few studies, tocotrienols inhibited cancer cell proliferation in both estrogen receptor positive and negative human breast cancer cells, with slight difference in potency.[55] In a comprehensive study investigating the effect of alpha-, delta- and gamma- tocotrienols on

proliferation and apoptosis in preneoplastic, neoplastic and malignant mouse mammary cells it was found that tocotrienols inhibited cell growth in a following rank order potency: delta-tocotrienol ≥ gamma-tocotrienol >alpha-tocotrienol. Recently two extensive reviews of epidemiological studies were published on relationships between vitamin E and breast cancer, where vitamin E dietary intake, serum levels of vitamin E or alpha-tocopherol levels in adipose tissue were taken into consideration. It was concluded that natural alpha-tocopherol from dietary sources with or without presence of other tocopherols and tocotrienols may provide women a modest protection against breast cancer.[56]

However, up to today, there is still scarce information available about differences in individual tocotrienols levels in diseased and healthy women. Moreover, so far there were only a few studies simultaneously monitoring all forms of natural tocopherols and tocotrienols in women diagnosed with breast cancer. One study reported detection of all four tocopherols along with alpha- and beta-tocotrienol in breast adipose tissue from 10 women with cancer. Unfortunately, this study did not include control subjects, thus no data for comparison is available. In another study only alpha- and gamma-tocopherol were analyzed with no report on other vitamin E isomers. The newest study on the other hand, reports analysis of all tocopherols and tocotrienols except the β-isomer, in breast adipose tissue in benign and malignant breast lumps. Still, no control was included in research and no plasma values were determined. Despite an increasing number of reports on the influence of tocotrienols on breast cancer cells a question about which tocotrienol isomer is the most potent inhibitor of cell proliferation is still not answered. Moreover, an interrelationship between each individual tocopherol and tocotrienol with respect to their concentration in the breast adipose tissue/plasma is not yet established. In other words we are still lacking an overall study where all natural vitamin E isomers would be researched simultaneously in breast cancer. The ability to noninvasive monitor the oxygenation state of individual tumor cells would have important implications for planning and evaluation therapy. The presence of hypoxia limits is the success of radiotherapy in animal tumor. Hypoxic cells impair the effectives of because of their cell-cycle kinetics. Residual malignant cells protected from these therapeutic modalities by hypoxia may regroup to cause local recurrence of the disease. Consequently, knowledge of the oxygenation status of clongenic cells within solid tumors before and during treatment would be extremely valuable. The spin–lattice relaxation rate ($1/T_1$) of PFOB will increases linearly with increasing oxygen concentration. In work, they explored, for the first time, the uptake of chitosan-coated PLGA PFOB nanoparticles and their potential as contrast agents for ^{19}FMRI.[57]

A fluorinated cobalt(II) complex serves as a turn-on ^{19}F MRI tracer for reactive oxygen species including H_2O_2. Upon oxidation with H_2O_2, the complex converts from paramagnetic high spin Co^{II} to diamagnetic low spin Co^{III} resulting in a chemical shift change and enhancement in ^{19}F NMR signal. Further, the oxidation can be reversed in the presence of reductant $Na_2S_2O_4$. ^{19}F MRI presents a ~2-3 fold enhancement in signal.[58] ^{19}F MRI T_1 mapping with diffusion-based multispectral (MS) analysis was introduced.[59] Giraudeau and coworkers present in vivo quantitative measurements of O_2 in the liver and spleen using ^{19}F MRI.[60] The next study demonstrates that ^{19}F MRI of hexafluorobenzene offers a feasible tool to measure regional O_2 concentrations of brain, kidney, liver, gut, muscle, and skin during inhalation of both 30 and 100% oxygen *in vivo*, and that hyperoxia significantly increases O_2 of multiple organs in a rat model.[61]

Oximetry of the human T-Lymphoblastoid (CEM) cells was measured using ^{19}F magnetic resonance imaging ^{19}F MRI.[36] ^{19}F MRI was used to evaluate oxygen concentration in the cell suspension and thus its viability Human gland mammary adenocarcinoma (MCF-7).[38] Tumor oxygenation has been shown to be an important indicator of therapeutic response. The pO_2 spike was detected even though few ($\sim 4\times10^4$) T cells actually ingress into the CNS and with minimal tumor shrinkage.[62] In ^{19}F MRI oximetry, a method used to image tumour hypoxia, perfluorocarbons serve as oxygenation markers.[63] The pO_2 maps were generated after direct intratumoral administration of a fluorine compound (hexafluorobenzene) whose relaxation rate ($1/T_1$) is proportional to the % O_2.[64]

^{19}F relaxation time

The T_1 and T_2 relaxation times of ^{19}F are relatively short, while the chemical shift is large (1000 ppm). Therefore we selected fluorine to label the Abs .[65] To allow clinical studies, *in vivo* concentrations of fluorine–containing metabolites must be larger than about 200 mol/g tissue to be detectable in reasonable measurements times 5-15 min at B_0=1-2 T. For animal studies at 7 T amount of 50 nmol/g can be detected within 30 min. In *ex vivo* studies 5-10 nmol / g can be detected within 1-2 hrs at 11.7 T.

Herein we provide an overview of the methods available for relaxation measurements in MRI. While standard magnetic resonance imaging can provide basic information regarding tumour location, its size and spread, the quantified MRI can evaluate the effectiveness of therapy. Of particular interest are changes in cells relaxivity which are correlated with cancer cells death. Medical MRI resolution of a few millimeters is typically adequate for proper diagnosis, however cell samples require much higher resolution. At the same time valuable physiological information can be extracted from a small cluster of cells, while quantitative investigations of dynamics of drug delivery and drug effects *ex vivo* was shown to be crucial for the development of effective therapy Therefore, there is a growing interest in using MRI for examination of the treated cells.

Fluorine-19 MR spectroscopy was used to monitor the anti-depressant drug fluoxetine (and its metabolite norfluoxetine) *in vivo* in the human brain. The individual T_1*s* varied from 149 to 386 ms, which was attributed in part to interindividual differences based on the reproducibility of a phantom T_1. The individual T_1 correlated weakly with approximate brain concentration.[66] Initial cell labeling strategies for MRI made use of contrast agents that influence the MR relaxation times T_1, T_2, T_2* and lead to an enhancement T_1 or depletion T_2* of signal where labeled cells are present.[67] The observed MRI image intensities were related to the NMR longitudinal and transverse relaxation times, and were found to depend on polymer structure and method of micellization.[68] The value of the *in vivo* spin-lattice relaxation time T_1 of the fluoride ions naturally accumulated in bone mineral has been determined to be 2.00 .[69]

Insufficient contrast between normal and diseased tissues requires the use of contrast agents. Cross-linked iron oxide (CLIO) and other iron oxide formulations affect T_2 primarily and lead to a decreased signal.[70] Many commercial PFC emulsions have been found to be nontoxic or do not cause any health problems other than tissue swelling. Perfluoropolyethylene glycol (PFPE, MW 1750) is a linear PFC that contains a large number of ^{19}F atoms per molecule for enhancing sensitivity . The center CF_2 groups can generate a strong peak (>0.9 at -92 ppm) that dominates 90% of its ^{19}F signal, whereas the end CF_2 groups yield a weak signal (<0.1 at -79 ppm) that is below the *in vivo* MRI detection limit. [71]

Spin-lattice relaxation times T_1 and T_1rho of fluorine atoms in solid dispersions were determined at various temperatures (-20 to 150 °C). Correlation time (tauc), which is a measure of rotational molecular mobility, was calculated from the observed T_1 or T_1rho value and that of the T_1 or T_1rho minimum, assuming that the relaxation mechanism of spin-lattice relaxation of FLF fluorine atoms does not change with temperature.[72] MRI of the ^{19}F longitudinal relaxation time T_1 of an inert fluorinated gas at thermal polarization. In contrast to hyperpolarized noble gases, with very long T_1*s*, the T_1 of SF_6 in mammal lungs is 0.8-1.3 ms. T_1 imaging of a phantom consisting of four different SF6/air mixtures with known T_1 values validates the modified Look-Locker T_1 imaging. [73]

Conclusions

^{19}F MRI alows for monitoring of ^{19}F containing compounds *in vitro* and *in vivo*. Abnormal oxygen content in adipose tissue indicative of cancer disorder also can be monitored with ^{19}F MRI. The number of newly synthetized ^{19}F containing compounds with medical application is increasing.

References

1. Hagmann WK. The many roles for fluorine in medicinal chemistry. J Med Chem. 2008;51:4359-69.
2. Heidelberger C, Chaudhuri NK, Daneberg P, Mooren D, Griesbach L, Duschinsky R. Fluorinated pyrimidines, a new class of tumour-inhibitory compounds. Nature. 1957;179:663-6.
3. Holland GN, Bottomley PA, Hinshaw WS. ^{19}F magnetic resonance imaging. J Mag Res. 1977;28:133-6.
4. Janjic JM, Ahrens ET. Fluorine-containing nanoemulsions for MRI cell tracking. Wiley Interdiscipl Rev Nanomed Nanobiotech. 2005;1:492-501.
5. Ahrens ET, Flores R, Xu H, Morel PA. *In vivo* imaging platform for tracking immunotherapeutic cells. Nature Biotechnol. 2005;23:983-7.
6. Ruiz-Cabello J, Barnett BP, Bottomley PA, Bulte JWM. Fluorine ^{19}F MRS and MRI in biomedicine. NMR in Biomed. 2011;24:114-29.
7. Kamm YJL, Heerschap A, van den Bergh EJ, Wagener DJT. ^{19}F-magnetic resonance spectroscopy in patients with liver metastases of colorectal cancer treated with 5-fluorouracil. Anti-Cancer Drugs. 2004;15:229-33.
8. Wang X, Chen J, Wang D, Dong S, Hao J, Hoffmann H. Monitoring the different micelle species and the slow kinetics of tetraethylammonium perfluorooctane-sulfonate by ^{19}F NMR spectroscopy. Advances in Colloid and Interface Science. 2017; DOI:10.1016/j.cis.2017.05.0169.
9. Drouza C, Dieronitou A, Hadjiadamou I, Stylianou M. Investigation of phenols activity in early stage oxidation of edible oils by electron paramagnetic resonance and ^{19}F NMR spectroscopies using novel lipid vanadium complexes as radical initiators. J Agric Food Chem. 2017;65:4942-51.
10. Hu H, Katyayan KK, Czeskis BA, Perkins EJ, Kulanthaivel P. Comparison between radioanalysis and ^{19}F Nuclear Magnetic Resonance Spectroscopy in the determination of mass balance, metabolism, and distribution of pefloxacin. Drug Metab Dispos. 2017;45:399-408.
11. Vints I, Gatenyo J, Rozen S. Fluorination of aryl boronic acids using acetyl hypofluorite made directly from diluted fluorine. J. Org. Chem. 2013;78:11794-7.
12. Gatenyo J, Hagooly Y, Vints I, Rozen S. Activation of a CH bond in polypyridine systems by acetyl hypofluorite made from F2. Organic & Biomol Chem. 2012;10:1856-60.
13. Liu Z, Shibata N, Takeuchi Y. Novel methods for the facile construction of 3,3-disubstituted and 3, 3-spiro-2H,4H--benzo[e]1,2-thiazine-1,1-diones: synthesis of (11S,12R, 14R)-2-fluoro-14-methyl-11-(methylethyl)spiro[4H-benzo[e]- 1, 2-thiazine-3,2'-cyclohexane]-1,1-dione, an agent for the electrophilic asymmetric fluorination of aryl ketone enolates. J Org Chem. 2000;65:7583-7.
14. Vora HU, Rovis T. N-Heterocyclic carbene catalyzed asymmetric hydration: direct synthesis of alpha-protio and alpha--deuterio alpha-chloro and alpha-fluoro carboxylic acids. J Am Chem Soc. 2010;132:2860-61.
15. Bennasar ML, Zulaica E, Juan C, Alonso Y, Bosch J. Addition of ester enolates to N-alkyl-2-fluoropyridinium salts: total synthesis of (+/-)-20-deoxycamptothecin and (+)-camptothecin. J Org Chem. 2002;67:7465-74.

16. Kamm YJ, Heerschap, van den Bergh EJ, Wagener DJ. ^{19}F-magnetic resonance spectroscopy in patients with liver metastases of colorectal cancer treated with 5-fluorouracil. Anticancer Drugs. 2004;15:229-33.
17. Stanosz M, Stanosz S, Puchalski A. An assessment of the influence of fluoride, modified transdermal replacement hormone therapy and supplement hormone therapy on unmanageable osteoporosis in postmenopausal women. J Elementol. 2009;14:545–51.
18. Lucas V, Sicre J, Laredo JD, Guérin C, Kuntz D, Dryll A. Spontaneous fracture of the femur neck in a female patient with osteoporosis treated with sodium fluoride, Rev Rhum Mal Osteoartic. 1990;5:545-8.
19. Zhang Q, Gladden L, Avalle P, Mantle M. In vitro quantitative ^{1}H and ^{19}F nuclear magneticresonance spectroscopy and imaging studies of fluvastatin™ in Lescol® XL tablets in a USP-IV dissolution cell. J Control Release. 2011;156:345-54.
20. White TE, Surles-Zeigler MC, Ford GD, et al. Bilateral gene interaction hierarchy analysis of the cell death gene response emphasizes the significance of cell cycle genes following unilateral traumatic brain injury. BMC Genomics. 2016;17:130.
21. Stolarczyk M, Apola A, Krzek J, Sajdak A. Validation of derivative spectrophotometry method for determination of active ingredients from neuroleptics in pharmaceutical preparations. Acta Pol Pharm Drug Res. 2009;66:351-6.
22. Bolo NR, Hode Y, Macher JP . Fluorine magnetic resonance spectroscopy measurement of brain fluvoxamine and fluoxetine in pediatric patients treated for pervasive developmental disorders. MAGMA. 2016:268-76.
23. Takeda T, Makita K, Ishikawa S, Kaneda K, Yokoyama K, Amaha K. Uptake and elimination of sevoflurane in rabbit tissues-an in vivo magnetic resonance spectroscopy study. Can J Anaesth. 2000;47:579-84.
24. Pablos AI, Escobar I, Albiñana S, Serrano O, Ferrari JM, de Tejada AH. Evaluation of an antibiotic intravenous to oral sequential therapy program. Pharmacoepidemiol drug safety. 2005;14:53–9.
25. Kane JM, Carson WH, Saha AR, et al. Efficacy and safety of aripiprazole and haloperidol versus placebo in patients with schizophrenia and schizoaffective disorder. J Clin Psych. 2002;63:763-71.
26. Sijens PE, Mostert JP , Irwan R , Potze JH , Oudkerk M, De Keyser J. Impact of fluoxetine on the human brain in multiple sclerosis as quantified by proton magnetic resonance spectroscopy and diffusion tensor imaging. Psychiatry Res. 2008;164:274-82.
27. Vakirlis E, Kastanis A, Ioannides D. Calcipotriol/betamethasone dipropionate in the treatment of psoriasis vulgaris. Ther Clin Risk Manag. 2008;4:141–8.
28. Lim YT, Cho MY, Kang JH, et al. Perfluorodecalin/[InGaP/ZnS quantum dots] nanoemulsions as ^{19}F MR/optical imaging nanoprobes for the labeling of phagocytic and nonphagocytic immune cells. Biomaterials. 2010;31:4964-71.
29. Bartusik D, Tomanek B, Lattová E, Perreault H, Fallone G. Combined treatment of human MCF-7 breast carcinoma with antibody, cationic lipid and hyaluronic acid using ex vivo assays. J Pharm Biomed Anal. 2010;51:192-201.
30. Ahrens ET1, Bulte JW. Tracking immune cells in vivo using magnetic resonance imaging. Nat Rev Immunol. 2013;13:755-63.
31. Managh AJ, Edwards SL, Bushell A, et al. Single cell tracking of gadolinium labeled CD4+ T cells by laser ablation inductively coupled plasma mass spectrometry. Anal Chem. 2013;85:10627-34.
32. Bartels M, Albert K. Detection of psychoactive drugs using ^{19}F MR spectroscopy. J Neural Transm Gen Sect. 1995;99:1-6.
33. Chubarova AS, Zakharovaa OD, Kovala OA, et al. Design of protein homocystamides with enhanced tumor uptake properties for ^{19}F magnetic resonance imaging. Bioorg Med Chem. 2015;23:6943–54.
34. Ahrens ET, Helfer BM, O'Hanlon CF, Schirda C. Clinical cell therapy imaging using a perfluorocarbon tracer and fluorine-19 MRI. Magn Reson Med. 2014;72:1696-701.
35. Amiri H, Srinivas M, Veltien A, van Uden MJ, de Vries IJ, Heerschap A. Cell tracking using 19F magnetic resonance imaging: Technical aspects and challenges towards clinical applications. Eur Radiol. 2015;25:726-35.
36. Waters EA, Chen K, Allen JS, Zhang H, Lanza GM, Wickline SA. Detection and quantification of angiogenesis in experimental valve disease with integrin-targeted nanoparticles and 19-fluorine MRI/MRS. J Card Magn Reson. 2008;10:43-5.
37. Higuchi M, Iwata N, Matsuba Y, Sato K, Sasamoto K, Saido TC. ^{19}F and ^{1}H MRI detection of amyloid beta plaques *in vivo.* Nat Neurosci. 2005;8:527-33.
38. Tooyama I, Yanagisawa D, Taguchi H, et al. Amyloid imaging using fluorine-19 magnetic resonance imaging ^{19}F MRI. Ageing Res Rev. 2016;30:85-94.
39. Matei E, Gronenborn AM. ^{19}F Paramagnetic Relaxation Enhancement: A Valuable Tool for Distance Measurements in Proteins. Angew Chem Int Ed Engl. 2016;55:150-4.
40. Neubauer AM, Caruthers SD, Hockett FD, et al. Fluorine cardiovascular magnetic resonance angiography in vivo at 1.5 T with perfluorocarbon nanoparticle contrast agents. J Cardiovasc Magn Reson. 2007;9:565-73.
41. Bartusik D, Tomanek B. Detection of fluorine labeled Herceptin using cellular ^{19}F MRI *ex vivo*. J Pharm Biomed Anal. 2010;51:894-900.
42. Bartusik D, Tomanek B, Siluk D, Kaliszan R. ^{19}F MRI of 3D CEM cells to study the effects of tocopherols and tocotrienols. J Pharm Biomed Anal. 2010;53:599-602.
43. Nobs L, Buchegger F, Gurny R, Allémann E. Surface modification of poly(lactic acid) nanoparticles by covalent attachment of thiol groups by means of three methods. Int J Pharm. 2003;250:327-37.
44. Bartusik D, Tomanek B, Siluk D, Kaliszan R, Fallone G. The application of ^{19}F magnetic resonance *ex vivo* imaging of

three-dimensional cultured breast cancer cells to study the effect of delta-tocopherol. Anal Biochem. 2009;387(2):315-7.
45. Clarkson PM. Antioxidants and Physical Performance. Crit Rev Food Sci Nutr. 1995;35:131-41.
46. Fleischauer AT, Simonsen N, Arab L. Antioxidant supplements and risk of breast cancer recurrence and breast cancer-related mortality among postmenopausal women. Nutr Cancer. 2003;46:15-22.
47. Meydani M, Evans WJ, Handelman G, et al. Protective effect of vitamin E on exercise-induced oxidative damage in young and older adults. Am J Physiol. 1993;264:992-8.
48. Buttner GR, Burns CP. Vitamin E slows the rate of free radical mediated lipid peroxidation in cells. Arch Biochem Biophys. 1996;334:261-7.
49. Hunter D A. prospective study of the Intake of Vitamins C, E, and A, and the risk of breast cancer. New Eng J Med. 1993;329:234-40.
50. Huang HY, Alberg AJ, Norkus EP, Hoffman SC, Comstock GW, Helzlsouer KJ. Prospective study of antioxidant micronutrients in the blood and the risk of developing prostate cancer. Am J Epidemiol. 2003;157:335-44.
51. Schwenke DC. Does lack of tocopherols and tocotrienols put women at increased risk of breast cancer? J Nutr Biochem. 2002;13:2-20.
52. Galli F, Stabile AM, Betti M, et al. The effect of alpha- and gamma-tocopherol and their carboxyethyl hydroxychroman metabolites on prostate cancer cell proliferation. Arch Biochem Biophys 2004;423:97-102.
53. Nesaretnam K, Ambra R, Selvaduray KR, Radhakrishnan A, Canall R, Virgill F. Tocotrienol-Rich Fraction from Palm Oil and Gene Expression in Human Breast Cancer Cells. Ann NY Acad Sci. 2004;1031:143-57.
54. Kashiwagi K, Harada K, Yano Y, et al. A redox-silent analogue of tocotrienol inhibits hypoxic adaptation of lung cancer cells. Biochem Biophys Res Commun. 2008;365:875-81.
55. Ditsch N, Mayer B, Rolle M. Estrogen receptor expression profile of disseminated epithelial tumor cells in bone marrow of breast cancer patients, Recent Results. Cancer Res. 2003;162:141-7.
56. McIntyre BS, Briski KP, Gapor A, Sylvester PW. Antiproliferative and apoptotic effects of tocopherols and tocotrienols on preneoplastic and neoplastic mouse mammary epithelial cells. Proc Soc Exp Biol Med. 2000;224:292-01.
57. Vu-Quanga H, Vinding MS, Xia D, et al. Chitosan-coated poly(lactic-co-glycolic acid) perfluorooctyl bromide nanoparticles for cell labeling in ^{19}F magnetic resonance imaging. Carbohydrate Polym. 2016;136:936–44.
58. Yu M, Xie D, Phan KP, Enriquez JS, Luci JJ, Que ML. A CoII complex for ^{19}F MRI-based detection of reactive oxygen species. Chem Commun. 2016;52:13885-88.
59. Shi Y, Oeh J, Eastham-Anderson J, et al. Mapping *in vivo* tumor oxygenation within viable tumor by ^{19}F MRI and multispectral analysis. Neoplasia. 2013;15(11):1241-50.
60. Giraudeau C, Djemaï B, Ghaly MA, et al. High sensitivity ^{19}F MRI of a perfluorooctyl bromide emulsion: application to a dynamic biodistribution study and oxygen tension mapping in the mouse liver and spleen. NMR Biomed. 2012;25:654-60.
61. Liu S, Shah SJ, Wilmes LJ, et al. Quantitative tissue oxygen measurement in multiple organs using ^{19}F MRI in a rat model. Magn Reson Med. 2011;66:1722-30.
62. Zhong J, Sakaki M, Okada H, Ahrens ET. *In vivo* intracellular oxygen dynamics in murine brain glioma and immunotherapeutic response of cytotoxic T cells observed by fluorine-19 magnetic resonance imaging. PLoS One. 2013;8:59479-83.
63. Baete SH, Vandecasteele J, De Deene Y. ^{19}F MRI oximetry: simulation of perfluorocarbon distribution impact. Phys Med Biol. 2011;56:2535-57.
64. Magat J, Jordan BF, Cron GO, Gallez B. Noninvasive mapping of spontaneous fluctuations in tumor oxygenation using ^{19}F MRI. Med Phys. 2010;37:5434-41.
65. Bartusik D, Tomanek B. Application of ^{19}F magnetic resonance to study the efficacy of fluorine labeled drugs in the three-dimensional cultured breast cancer cells. Arch Biochem and Biophys. 2010;493:234–41.
66. Komoroski RA, Newton JE, Cardwell D, Sprigg J, Pearce J, Karson CN. *In vivo* ^{19}F spin relaxation and localized spectroscopy of fluoxetine in human brain. Magn Reson Med. 1994;31:204-11.
67. Waiczies H, Guenther M, Skodowski J, et al. Monitoring dendritic cell migration using ^{19}F/^{1}H magnetic resonance imaging. J Vis Exp. 2013;73:e50251. doi: 10.3791/50251.
68. Peng H, Blakey I, Dargaville B, Rasoul F, Rose S, Whittaker AK. Synthesis and evaluation of partly fluorinated block copolymers as MRI imaging agents. Biomacromolecules. 2009;10:374-81.
69. Code RF, Harrison JE, McNeill KG, Szyjkowski M. *In vivo* ^{19}F spin relaxation in index finger bones. Magn Reson Med. 1990;13:358-69.
70. Chen J, Pan H, Lanza GM, Wickline SA. Perfluorocarbon nanoparticles for physiological and molecular imaging and therapy. Adv Chronic Kidney Dis. 2013:20:466-78.
71. Winter PM. Perfluorocarbon Nanoparticles: Evolution of a Multimodality and Multifunctional Imaging Agent. Scintifica. 2014; Article ID 746574, 1-10.
72. Aso Y, Yoshioka S, Miyazaki T, Kawanishi T. Feasibility of ^{19}F NMR for assessing the molecular mobility of flufenamic acid in solid dispersions. Chem Pharm Bull (Tokyo). 2009;57:61-4.
73. Adolphi NL, Kuethe DO. Quantitative mapping of ventilation-perfusion ratios in lungs by ^{19}F MR imaging of T_1 of inert fluorinated gases. Magn Reson Med. 2008;59:739-46.